Published in final edited form as:

Magn Reson Med. 2018 January ; 79(1): 31–40. doi:10.1002/mrm.26683.

Tailored Spiral In-Out Spectral-Spatial Water Suppression Pulses for Magnetic Resonance Spectroscopic Imaging

Jun Ma[1,2], **Carrie Wismans**[3], **Zhipeng Cao**[1,2], **Dennis W.J. Klomp**[3], **Jannie P. Wijnen**[3], and **William A. Grissom**[*,1,2]

[1]Vanderbilt University Institute of Imaging Science, Nashville, TN, United States [2]Department of Biomedical Engineering, Vanderbilt University, Nashville, TN, United States [3]Department of Radiology, University Medical Centre Utrecht, Utrecht, the Netherlands

Abstract

Purpose—To develop short water suppression sequences for 7 Tesla magnetic resonance spectroscopic imaging (MRSI), with mitigation of subject-specific transmit RF field (B_1^+) inhomogeneity.

Methods—Patient-tailored spiral in-out spectral-spatial (SPSP) saturation pulses were designed for a three-pulse WET water suppression sequence. The pulses' identical spatial subpulses were designed using patient-specific B_1^+ maps and a spiral in-out excitation k-space trajectory. The subpulse train was weighted by a spectral envelope that was root-flipped to minimize peak RF demand. The pulses were validated in *in vivo* experiments that acquired high resolution MRSI data, using a crusher coil for fast lipid suppression. Residual water signals and MR spectra were compared between the proposed tailored sequence and a conventional WET sequence.

Results—Replacing conventional spectrally-selective pulses with tailored SPSP pulses reduced mean water residual from 5.88% to 2.52% (57% improvement). Pulse design time was less then 0.4 seconds. The pulses' SAR were compatible with MRSI TRs under 300 ms, which enabled spectra of fine in plane spatial resolution (5 mm) with good quality to be measured in 7.5 minutes.

Conclusion—Tailored SPSP water suppression enables efficient high resolution MRSI in the brain.

Keywords

Spectroscopy; RF pulses; Ultra-high field MRI; RF pulse design; Selective excitation; Optimization

Introduction

Magnetic resonance spectroscopic imaging (MRSI) enables *in vivo* studies of local metabolite distributions and changes. Neurologists and neuroscientists are often interested in

[*]Corresponding author: Will Grissom, Department of Biomedical Engineering, Vanderbilt University, 5824 Stevenson Center, Nashville, TN 37235 USA, will.grissom@vanderbilt.edu, Twitter: @wgrissom.

metabolic changes in specific regions with small volumes and irregular shapes. MRSI with high spatial resolution is therefore desirable to avoid partial volume effects and obtain measurements that closely follow anatomies of interest [1, 2]. The increased signal-to-noise ratio at ultra-high field strengths (7T and above) has the potential to enable MRSI with significantly finer spatial resolution than is possible at lower field strengths. However, since (without using complex acceleration techniques) each k-space location requires one FID measurement, acquisition matrices of 32×32 or higher only have clinically acceptable measurement times (5–10 minutes) when the TR is short (≤300ms), corresponding to a high SNR per unit time. The short TR requirement poses a challenge for performing water and fat suppression, which is necessary since metabolite signals of low concentration can be overwhelmed by those very large signals. Conventional water and fat suppression techniques for MRSI require considerable sequence time, and are not compatible with fast scanning. Recently, we introduced fast fat suppression for brain MRSI using a crusher gradient coil [3]. Therefore, short and effective water suppression is the remaining challenge that prevents the use of short TRs for high resolution MRSI at ultra-high field.

Water suppression is based on differences in the NMR properties of water and metabolites, and most methods are based on differences in longitudinal relaxation time (T_1) and chemical shift. In relaxation-based water suppression, water signal is selectively inverted, and metabolite signal is excited and measured when water's longitudinal magnetization crosses zero [4–8]. These methods are currently the most effective at high field due to robustness to B_1^+ inhomogeneity, since selective adiabatic pulses can be used for inversion [8]. However, since the T_1 of water is approximately one second, these methods' duration are on the order of one second. Furthermore, double adiabatic inversion is most often used to overcome T_1 variations [7], but it comes with a specific absorption rate (SAR) penalty that increases the minimum TR that can be used. For example, we calculated that the SAR of a double adiabatic inversion sequence is approximately 10×higher than the tailored spectral-spatial (SPSP) sequence proposed here.

Spectrally-selective water suppression methods based primarily on differences in chemical shift are more time-efficient than relaxation-based methods, since one does not need to wait for longitudinal water magnetization to cross zero. The WET sequence [9] (Figure 2) is one of the most commonly used spectrally-selective methods, and can be implemented with a short duration (100–200 ms) which makes it compatible with high-resolution MRSI. It is a three-pulse extension of the CHESS sequence [10], which comprises a spectrally-selective 90 degree excitation pulse (boxed in Figure 2) followed by a spoiler gradient, to selectively excite and dephase water magnetization. The CHESS sequence is sensitive to B_1^+ inhomogeneity since imperfect 90 degree excitation leaves partial longitudinal water magnetization. The WET sequence mitigates this sensitivity somewhat by using three consecutive RF and gradient pairs with variable flip angles. However, it remains quite sensitive to the levels of B_1^+ inhomogeneity encountered at 7T. Another more effective extension of CHESS is the seven-pulse VAPOR sequence [11], but VAPOR has a duration of more than 700 ms that renders it incompatible with fast high-resolution MRSI. Unlike inversion-based water suppression, the B_1^+ sensitivity of CHESS and its extensions cannot be addressed by replacing the conventional spectrally-selective RF pulses with adiabatic

pulses, since there are no suitable spectrally-selective adiabatic excitation pulses with low SAR. In recent years, subject-tailored RF pulses with lower SAR than adiabatic pulses have been developed for slice-selective and 3D excitations in high field MRI [12–18]. In those methods, a subject's B_1^+ distribution is measured and used to design multidimensional pulses that produce higher flip angles in regions with low B_1^+, and vice versa. To our knowledge however, tailored RF methods have not been developed for water suppression in MRSI.

Here we propose subject-tailored spiral in-out SPSP water suppression pulses that are designed using a subject's B_1^+ map in the slice of interest. The pulses replace the conventional spectrally-selective pulses in the WET sequence. An SPSP pulse comprises a train of identical tailored spatial subpulses that are weighted by a spectral envelope. Previously, three-dimensional (two spatial dimensions plus the spectral dimension) SPSP pulses have been implemented using trains of spiral-in or spiral-out subpulses [19, 20]. We propose the use of spiral in-out spatial subpulses, which are designed to produce uniform flip angles over the slice of interest. The spectral envelope is designed to be spectrally-selective for water, and is root-flipped to minimize peak RF amplitude [21–23]. In the following, we describe a computationally efficient procedure to design the SPSP pulses, and compare the spiral in-out subpulse trajectory to the spiral-in trajectory that is conventionally used for three-dimensional SPSP excitations. We then present an evaluation of the SPSP pulses in MRSI scans of human volunteers at 7T, and demonstrate improved water suppression and spectral quality compared to those obtained with a conventional WET sequence with matched spectral parameters.

Methods

Spiral In-Out Spectral-Spatial Pulse Design

Overview—Figure 1 illustrates the overall design procedure. An SPSP pulse comprises a train of identical tailored spatial subpulses that are weighted by a spectral envelope. The identical spatial subpulses are designed via magnitude least-squares optimization [24] using a patient-specific B_1^+ map and a pre-emphasized spiral in-out excitation k-space trajectory [25]. The subpulse train is then weighted by a spectral envelope that is designed using the Shinnar-Le Roux (SLR) algorithm [26], with root-flipping to minimize peak RF demand [21–23, 27]. The spectral field-of-view (FOV) dictates the duration of the spiral in-out subpulses, but otherwise the spectral and spatial pulse designs are decoupled. MATLAB (The Mathworks, Natick, MA, USA) code for the algorithm in one of the imaged subjects can be downloaded from https://bitbucket.org/wgrissom/tailoredwater-suppression-paper.

Spectral Envelope Design—The spectral design parameters are derived from a conventional WET sequence for water suppression at 7T (Figure 2), which uses three 32 ms linear phase spectrally selective pulses, with flip angles of 80, 80, and 145 degrees, all with the same phase [9]. The pulses have identical time-bandwidth-products of 9.6, and a pass-plus transition-band width of 1 ppm (300 Hz). Figure 3 illustrates the spectral characteristics of the tailored SPSP pulses, which are designed for the same flip angles and spectral characteristics as the conventional WET pulses. However, since an SPSP pulse's spectral

envelope is coarsely sampled by its subpulses, it will produce passband replicas, which must not interfere with the metabolites of interest, which are between 0.5 ppm (150 Hz) and 4.7 ppm (1400 Hz). Therefore, as shown in Figure 3 the spectral FOV is set to 5.2 ppm (1550 Hz), with a 1 ppm- (300 Hz) wide passband plus transition bandwidth, and a stop- (metabolite) bandwidth of 4.2 ppm (1250 Hz).

The spectral envelope is designed using the SLR algorithm, and is chosen to be minimum-phase rather than linear phase, since the excited phase profile is unimportant in signal saturation, and since a minimum-phase pulse has narrower transition bands than a linear-phase pulse of the same time-bandwidth product [26]. This is leveraged to shorten the pulse durations to 26 ms with a time-bandwidth product of 6.23, which produces spectral profiles of equivalent sharpness (54 Hz transition widths) to the 32 ms, time-bandwidth 9.6 linear-phase pulses used in the conventional WET sequence. Together, their 26 ms duration and the target 1550 Hz spectral FOV determine that the pulses comprise 41 samples/subpulses of duration 0.645 ms. The pulses are designed with 0.1% passband ripple and 1% stopband ripple. Once designed, an exhaustive search of the pulses' minimum-phase beta polynomial passband root-flip combinations is then performed to minimize peak RF amplitude while maintaining the excitation profile's magnitude. To replace the three conventional spectral pulses in the 80-80-145 WET sequence, two spectral envelopes are designed with 80 and 145 degree flip angles, and the final SPSP pulses are constructed using the same spatial subpulse whose design is detailed below.

Spatial Subpulse Design—For each subject, a single 0.645 ms spiral in-out spatial subpulse is designed to produce a uniform flip angle pattern over the brain slice of interest. The design procedure is illustrated in Figure 4. First, a B_1^+ map is measured in the slice with a 32×32 matrix size, and masked to remove out-of-brain voxels. The measurements are made using the Bloch-Siegert method with optimized encoding pulses [28, 29], a 32×32 image matrix and 22 cm^2 FOV. A mask of spatial locations within the brain is obtained using an ROI selection tool for the pulse designs.

Given the map, the spatial locations and the spiral in-out trajectory $\vec{k}(t)$ (described further below), a small-tip-angle excitation system matrix $\boldsymbol{A}$ is constructed with elements [30, 31]:

$$a_{i,j}=\iota\gamma\Delta_t\tilde{B}_1^+(\vec{x}_i)\,e^{\iota\vec{k}(t_j)\cdot\vec{x}_i}, \quad [1]$$

where $\iota=\sqrt{-1}$, γ is the gyromagnetic ratio, Δ_t is the dwell time for the design (6.4 μs on the Philips 7T Achieva scanner (Philips Healthcare, Cleveland, Ohio, USA)), and $\tilde{B}_1^+(\vec{x}_i)$ is the median-normalized B_1^+ field at $\vec{x}_i$. Off-resonance is neglected due to the very short duration of the pulses. The B_1^+ map median normalization stabilizes RF power regularization between subjects; the median is re-applied to the pulses after they are designed. Given the relatively small dimensions of this matrix (approximately 400 spatial locations after masking, and approximately 100 time points), the pulses can be efficiently computed using the RF power-regularized pseudo-inverse of the $\boldsymbol{A}$ matrix, given by:

$$\boldsymbol{A}^{\dagger}=\left(\boldsymbol{A}^{H}\boldsymbol{A}+\frac{\lambda}{N}\boldsymbol{I}\right)^{-1}\boldsymbol{A}^{H}. \quad [2]$$

The RF power regularization parameter λ is normalized by the number of voxels in the masked brain B_1^+ map (N), so that RF power regularization is approximately independent of B_1^+ map resolution and the number of brain voxels.

A spiral in-out k-space trajectory was chosen for two dimensional spatial encoding in the subpulses. To our knowledge, this trajectory has not been previously used for SPSP excitation. Although it does not reach as fine a spatial resolution as a spiral-in or spiral-out trajectory of the same duration, it has three potential advantages. First, since it visits same k-space positions twice, RF amplitude is lower. Second, since it is inherently refocused, the RF duty cycle can be close to 100% (meaning that RF is played for almost the entire subpulse duration), while a larger portion of the duty cycle is wasted on the prewinder or rewinder of a spiral-in or spiral-out trajectory (Figure 5a). Third, when used for image encoding, spiral in-out readouts have been demonstrated to be robust to off-resonance, since off-resonance phase accrual cancels to first order when signals during spiral in and spiral out are summed [32]. We performed simulations (described below) to compare spiral in-out to spiral-in subpulses for the present SPSP application, and to evaluate whether the off-resonance advantage of spiral in-out trajectories extends to RF excitation. The excitation field-of-view (XFOV) and resolution for all spiral in-out subpulse designs were 10 cm and 3.3 cm, respectively, and the trajectories were slew-rate limited to 180 mT/m/ms. Before pulse design, the spiral gradient waveforms were pre-emphasized using an iterative gradient pre-distortion method [25] to reduce errors from eddy currents, group delay, and the scanner's own pre-emphasis which is optimized for trapezoidal waveforms. All gradient waveform measurements were made using the method of Ref. [33]. The pre-emphasis was performed once in a phantom, with a regularization parameter of 0.01, and an update step size of 0.5 [25]. The RMS error of the gradient waveforms decreased 67% with pre-emphasis. The final measured pre-emphasized gradient waveforms are used for pulse design, and are centered at DC, to enable zero-phase target profile initialization in the magnitude-least-squares optimization problem described next.

Since the phase of the excitation profile is unimportant, a magnitude-least-squares optimization is used to achieve a better magnitude profile [24]. This is implemented using a variable projection approach, in which the target excitation pattern is updated at each iteration so that its phase equals the phase of the previous iteration's realized excitation pattern, as:

$$d_i \leftarrow e^{\iota\angle\{\boldsymbol{Ab}\}_i}, \quad [3]$$

where $\boldsymbol{b}$ was the previous iteration's RF pulse vector. For the first iteration, the target pattern was initialized to a vector of ones (no phase). Iterations stop when the cost function (i.e., the sum of squared excitation error and RF power regularization) decreases by less than 1% of

its previous value. The final pulse is constructed by replicating the spatial subpulse 41 times and weighting each replica by its position in the spectral envelope. The overall pulse design was implemented on a Core i7 laptop (Intel Corporation, Santa Clara, CA, USA), and took 0.4 seconds on average.

Simulations

A simulation was performed to compare the robustness of spatial subpulses designed with spiral in-out and spiral-in trajectories to resonance frequency offset. Pulses were designed as described above (i.e., without incorporating off-resonance in the design) with a subject's measured B_1^+ map, and with either a spiral in-out or spiral-in trajectory (Figure 5a), with the same durations. Then the pulses' small-tip-angle excitation patterns were calculated for frequency offsets ranging from −1500 Hz to +1500 Hz. In a second simulation, the sensitivity of subpulse excitation error and SPSP pulse SAR (quantified as the minimum TR allowed for the MRSI sequence) to the regularization parameter λ was also evaluated across 28 subjects, to justify the selected regularization parameter ($10^{2.5}$). Finally, the peak RF amplitudes of pulses designed with and without spectral envelope root-flipping were compared.

In Vivo MRSI Experiments

The tailored spiral-in-out SPSP water suppression pulses were inserted into the WET portion of an MRSI sequence and used to scan healthy subjects at 7T. Subject participation was approved by Institutional Review Board of the University Medical Centre Utrecht, after providing informed consent. The slice of interest was selected for a study on amyotrophic lateral sclerosis for the investigation of brain metabolism in brain areas affected by the disease. Areas of interest included: the banks of the left superior temporal sulcus, left cuneus, left inferior parietal area, left isthmus cingulate area, the banks of the right superior temporal sulcus, right pars triangularis area, left caudatus and left putamen. The selected slice was imaged with a 22×22 cm^2 FOV and 0.5×0.5 cm^2 spatial resolution. The MRSI acquisition bandwidth was 3000 Hz, the spectral resolution was 5.86 Hz/point, and the FID excitation flip angle was 35 degrees. Automatic image-based second-order shimming was applied. Skull fat was suppressed by a crusher coil [3] using a 1.2 ms current pulse played 0.8 ms after FID excitation. The crusher coil is an actively switchable coil that generates a very local distortion of the B_0 magnetic field in the skull and skin. The depth of spoiling can be adjusted up to approximately 3 cm from the coil by adjusting the driving current. This was done on a per-subject basis, by visual inspection of the suppression area on a fast proton density weighted scan. The crusher coil was interfaced to one of the unused B_0 shim amplifiers of the 7T scanner and switched during the sequences by means of a commercially available dynamic shim update unit (Load & Go Real Time Shims, Resonance Research Inc, Billerica, MA, USA). The same TR was used for all subjects to maintain consistent T_1 weighting, and was set to 300 ms based on previous experience with the range of scanner-enforced minimum TR's in different subjects for the conventional WET-MRSI sequence, which depends on the spectral resolution and the scanner's subject-dependent SAR calculation. This TR corresponded to a total scan time of 7.5 minutes. Measurements were done with no water suppression, with conventional WET water suppression, and with the

proposed water suppression. To compare the quality of water suppression between the two methods, for each voxel, signal in the water band was summed, and then normalized by the measured water signal with no suppression. Metabolite spectra were generated with and without post-processing removal of water signal. The post-processing steps included fitting the unsuppressed spectra to the water-suppressed spectra in each voxel and subtracting the fit from the water-suppressed spectra, followed by SVD-based water filtering [34].

Results

Simulations

Figure 5 shows the comparison between spatial subpulses designed using spiral-in and spiral in-out trajectories. The spiral-in pulse has approximately 24% finer spatial resolution (2.5 cm) than the spiral in-out pulse (3.3 cm) (Figure 5a) and has lower on-resonance root-mean-square (RMS) excitation error (3% versus 4.45%), but the spiral in-out pulse has 47% lower peak amplitude and 40% lower SAR since it visits the center of k-space twice (Figure 5b). The spiral-in pulse spends 26% (0.168 ms) of the possible RF duty cycle on its prewinder (the prewinder is the initial linear ramp of the spiral-in k_x waveform in Figure 5a), compared to 10% (0.065 ms) for the spiral in-out pulse. Figure 5c shows that the spiral in-out pulse is robust to up to approximately 500 Hz frequency offset (with root-mean-square (RMS) error less than 6%), while the spiral in pulse's error increases rapidly with frequency offset and exceeds that of the spiral in-out pulse at ±100 Hz, reaching an RMS error of approximately 15% at ±500 Hz offset. Figure 5d shows simulated excitation error patterns at 0 and 500 Hz, where the very large errors of the spiral in pulse can be appreciated at +500 Hz.

Simulated spatial subpulse RMS excitation error and overall sequence TR are plotted in Figure 6 as a function of the RF power regularization parameter λ. Each line represents pulses designed for one of the 28 subjects. To meet the sub-300 ms TR constraint, based on Figure 6 the λ for all scans was chosen to be $10^{2.5}$. At this value, the RMSE's of the spatial subpulse designs were under 36% for all subjects, as shown in Figure 6b.

As shown in Figure 7, root-flipping the 145 degree spectral envelope (black) reduced peak amplitude by 50% compared to the initial minimum-phase SLR envelope (gray). The 80 degree pulse peak amplitude was similarly reduced 43% with root flipping (not shown). The peak amplitude of the 145 degree pulse with the minimum-phase envelope was 20.3 μT, which exceeds the peak RF limit of many head and body coils that have upper limits of 13–18 μT. Without root-flipping, the peak RF demand of the 145 degree pulse exceeded 18 μT in 8 of the 28 subjects from Figure 6.

Experiments

Figure 8 compares water suppression performance between conventional WET and the proposed sequence in five healthy subjects. Figure 8a shows simulated normalized single subpulse excitation patterns and measured water residual maps for each subject, as well as the corresponding B_0 maps. The single subpulse patterns are equal to the B_1^+ maps for WET, since it uses spectrally-selective pulses only. The spiral subpulse flip angle maps generally reduced flip angles in the middle of the brain, and increased flip angles on the sides. This

improvement in flip angle homogeneity primarily resulted in reduced water residuals on the left and right sides of the brain, since the scanner adjusts its transmit gain so that the target field strength is met in the middle of the brain. In Subject 2, B_0 field distortions above the sinuses caused the water signal frequency to shift out of the pulses' passband, resulting in high water residuals for both methods there. Figure 8b compares water residual histograms from all five subjects (3944 total voxels). The third histogram is the direct subtraction of the previous two, which shows that the tailored SPSP sequence resulted in a significant increase in pixels with water residual under 3%. Figure 8c shows the corresponding mean and max water residuals for the five subjects. The proposed sequence largely reduced mean and max water residuals in each subject, and the overall mean water residual was reduced from 5.88% to 2.52%, a 57% decrease.

The left image in Figure 9 shows MR spectra from Subject 3 using the proposed sequence for water suppression, overlaid on the corresponding anatomical image. The skull fat around most of the brain was suppressed by the crusher coil and only very limited fat signal remained, though large lipid signals remained in the front of the brain (as indicated in the Figure), where the subject's head was not close enough to the conductors of the rigid crusher coil. Figure 9 also shows the enlarged MR spectra in three boxed voxels, which had the best, average (most common), and worst improvement in residual water signal. All y-axis are unit-less signal intensity and scaled the same. As shown in Figure 8, the best improvement was a result of the proposed method's robustness to B_1^+ inhomogeneity at the lateral regions, and the worst improvement was a result of similarly good water suppression from both methods due to strong B_1^+ in the middle of the brain. The spectra obtained using different water suppression methods were compared, before and after further water removal by post-processing. As shown in the spectra before water removal in the best and average improvement cases, conventional WET resulted in much larger water line widths and larger water side bands, which remained after water removal by post-processing and degraded the metabolite spectrum in the best improvement case. The MR spectra obtained with proposed method before and after water removal were of good quality in all three cases. Overall this example illustrates that the tailored pulses reduce the need for an additional unsuppressed acquisition to fully remove water signal, and improve the likelihood of successful post-processing.

Discussion

A short and effective water suppression method was proposed to enable high resolution MRSI at ultra-high field. The method replaces the conventional spectrally-selective saturation pulses used in the three-pulse WET water suppression sequence with patient-tailored spiral in-out SPSP saturation pulses, to provide robust and short water suppression in the presence of large B_1^+ inhomogeneities. The spiral in-out trajectory used in the pulses, combined with root-flipping, resulted in low peak RF amplitudes and acceptable SAR, even for flip angles of 145 degrees. The pulses were designed using a computationally efficient (<0.4 seconds total design time) separable method in which the short spatial subpulses were first designed using an iterative magnitude-least-squares method based on a precomputed regularized matrix pseudo-inverse, and were then duplicated to form a train that was

weighted by the root-flipped spectral envelope. The resulting patient-tailored water suppression sequence was validated in *in vivo* experiments, in which the pulses' SAR were compatible with TRs under 300 ms and enabled MRSI data with fine in plane spatial resolution (5 mm) and good spectral quality to be measured in 7.5 minutes, with a crusher coil for fast lipid suppression. Averaged across 5 subjects, the proposed method reduced mean water residual from 5.88% to 2.52% (57% improvement) compared to conventional WET.

We further showed that spiral in-out RF pulses are less sensitive to off-resonance, have lower power, and have a higher RF duty cycle than spiral-in pulses of the same duration and XFOV. Since the spiral in-out trajectory was slew-rate limited and its total duration was fixed at 0.645 ms, its XFOV and its initial rotation angle were the only parameters that could be tuned; Supporting Figure S1 shows that spatial subpulse excitation error is relatively insensitive to XFOV and that the chosen XFOV of 10 cm was close to the best value of 12 cm, when error was averaged across 28 subjects. The average best rotation angle for an XFOV of 10 cm was also used in all experiments. As shown in Figure 8a, the spiral in-out pulses reduced flip angle inhomogeneity primarily by mitigating the central brightening effect in the middle of the brain, and flip angles were typically lower on the sides of the brain due to the higher frequency B_1^+ variations there.

While the proposed method addressed WET's sensitivity to B_1^+ inhomogeneity, it remained sensitive to off-resonance that pushed water out of the spectral envelope's passband. This subject-and slice position-dependent effect was especially evident in the front of the brain above the sinuses. It could be reduced using shim coil arrays or combined RF coil/shim arrays [35–38]. An alternative and complementary approach would be to perform a full iterative waveform design (instead of the separable method used here) that incorporates a measured off-resonance map, to try to generate a different spectral profile at each spatial location that is centered on the local water peak [39–41]. However, Supporting Figure S2 shows that directly applying full waveform design with off-resonance compensation to our current experimental setup does not provide a clear improvement in pulse performance. This is due to the limited spatial encoding that is possible within the very short subpulse duration (0.645 ms) which is imposed by the spectral FOV. A full waveform design would also require more sophisticated and longer computation than the separable method used here. However, we anticipate that parallel excitation could enable sufficiently fine spatial encoding to make off-resonance compensation feasible, and it could also enable more complete mitigation of B_1^+ inhomogeneity [31, 41–43]. This will be the focus of future work.

In this work, SPSP pulses were developed to suppress water in MRSI with robustness to B_1^+ inhomogeneity, and were followed by an excitation and signal readout that were not spectrally-selective. B_1^+ inhomogeneity-robust adiabatic SPSP pulses have been previously used for refocusing in volume-localized MRSI sequences [44–51]. One recent example is the Semiadiabatic Spectral-Spatial Spectroscopic Imaging (SASSI) sequence which uses two adiabatic SPSP refocusing pulses to achieve insensitivity to B_1^+ inhomogeneity, along with a linear-phase SPSP pulse for excitation [51]. An advantage of this sequence is that since it uses volume localization it can potentially eliminate all water and lipid signals. The main

drawbacks of SASSI and other adiabatic PRESS sequences are their smaller spectral bandwidths and their longer TR's due to the high SAR of their at least two refocusing pulses, so matrices of, e.g., 44×44 as used in the present study would require longer scan times. It may however be useful to apply the proposed tailored spiral in-out SPSP water suppression sequence to further improve water suppression in SASSI and related sequences. If another method can be used for slice-selection, it may also be possible to use tailored spiral in-out SPSP pulses for spectrally-selective excitation in pulse-and-acquire phase-encoded MRSI, though their power would increase due to the approximately 4× broader excitation bandwidth compared to when they are designed to only excite water.

Conclusion

We have proposed and validated spiral in-out spectral-spatial tailored RF pulses for water suppression in high resolution MRSI. Compared to the conventional WET method, the pulses reduced mean residual water signal by 57%.

Supplementary Material

Refer to Web version on PubMed Central for supplementary material.

Acknowledgments

This work was supported by NIH R01 EB016695.

References

1. Henning A, Fuchs A, Murdoch JB, Boesiger P. Slice-selective FID acquisition, localized by outer volume suppression (FIDLOVS) for 1H-MRSI of the human brain at 7 T with minimal signal loss. NMR Biomed. 2009; 22:683–696. [PubMed: 19259944]
2. Bogner W, Gruber S, Trattnig S, Chmelik M. High-resolution mapping of human brain metabolites by free induction decay (1)H MRSI at 7 T. NMR in Biomedicine. 2012; 25:873–882. [PubMed: 22190245]
3. Boer VO, van de Lindt T, Luijten PR, Klomp DW. Lipid suppression for brain MRI and MRSI by means of a dedicated crusher coil. Magn Reson Med. 2015; 73:2062–2068. [PubMed: 24947343]
4. Patt SL, Sykes BD. Water eliminated Fourier transform NMR spectroscopy. J Chem Phys. 1972; 56:3182–3184.
5. Bydder G, Young I. MR imaging: clinical use of the inversion recovery sequence. J Comput Assist Tomogr. 1985; 9:659–675. [PubMed: 2991345]
6. Hajnal JV, De Coene B, Lewis PD, Baudouin CJ, Cowan FM, Pennock JM, Young IR, Bydder GM. High signal regions in normal white matter shown by heavily T2-weighted CSF nulled IR sequences. J Comput Assist Tomogr. 1992; 16:506–513. [PubMed: 1629405]
7. Shen JF, Saunders JK. Double inversion recovery improves water suppression in vivo. Magn Reson Med. 1993; 29:540–542. [PubMed: 8385261]
8. Hajnal JV, Oatridge A, Herlihy AH, Bydder GM. Reduction of CSF artifacts on FLAIR images by using adiabatic inversion pulses. Am J Neuroradiol. 2001; 22:317–322. [PubMed: 11156777]
9. Ogg RJ, Kingsley R, Taylor JS. WET, a T_1- and B_1-insensitive water-suppression method for in vivo localized 1H NMR spectroscopy. J Magn Reson, Ser B. 1994; 104:1–10. [PubMed: 8025810]
10. Haase A, Frahm J, Hanicke W, Matthaei D. 1H NMR chemical shift selective (CHESS) imaging. Phys Med Bio. 1985; 30:341. [PubMed: 4001160]
11. Tkáč I, Starčuk Z, Choi IY, Gruetter R. In vivo 1H NMR spectroscopy of rat brain at 1 ms echo time. Magn Reson Med. 1999; 41:649–656. [PubMed: 10332839]

12. Saekho S, Yip CY, Noll DC, Boada FE, Stenger VA. Fast-kz three-dimensional tailored radiofrequency pulse for reduced B1 inhomogeneity. Magn Reson Med. 2006; 55:719–724. [PubMed: 16526012]
13. Zhang Z, Yip CY, Grissom W, Noll DC, Boada FE, Stenger VA. Reduction of transmitter B1 inhomogeneity with transmit SENSE slice-select pulses. Magn Reson Med. 2007; 57:842–847. [PubMed: 17457863]
14. Setsompop K, Alagappan V, Zelinski AC, Potthast A, Fontius U, Hebrank F, Schmitt F, Wald LL, Adalsteinsson E. High-flip-angle slice-selective parallel RF transmission with 8 channels at 7T. J Magn Reson. 2008; 195:76–84. [PubMed: 18799336]
15. Setsompop K, Alagappan V, Gagoski B, Witzel T, Polimeni J, Potthast A, Hebrank F, Fontius U, Schmitt F, Wald L, Adalsteinsson E. Slice-selective RF pulses for in vivo B_1+ inhomogeneity mitigation at 7 Tesla using parallel RF excitation with a 16-element coil. Magn Reson Med. 2008; 60:1422–1432. [PubMed: 19025908]
16. Grissom WA, Khalighi MM, Sacolick LI, Rutt BK, Vogel MW. Small-tip-angle spokes pulse design using interleaved greedy and local optimization methods. Magn Reson Med. 2012; 68:1553–1562. [PubMed: 22392822]
17. Cloos MA, Boulant N, Luong M, Ferrand G, Giacomini E, Le Bihan D, Amadon A. k_T-Points: Short three-dimensional tailored RF pulses for flip-angle homogenization over an extended volume. Magn Reson Med. 2011; 67:72–80. [PubMed: 21590724]
18. Cao Z, Donahue MJ, Ma J, Grissom WA. Joint design of large-tip-angle parallel RF pulses and blipped gradient trajectories. Magn Reson Med. 2016; 75:1198–1208. [PubMed: 25916408]
19. Morrell G, Macovski A. Three-dimensional spectral-spatial excitation. Magn Reson Med. 1997; 37:378–386. [PubMed: 9055228]
20. Deng W, Stenger VA. A three-dimensional variable-density spiral spatial-spectral RF pulse with rotated gradients. Magn Reson Med. 2010; 63:828–34. [PubMed: 20187190]
21. Shinnar M. Reduced power selective excitation radio frequency pulses. Magn Reson Med. 1994; 32:658–660. [PubMed: 7808268]
22. Pickup S, Ding X. Pulses with fixed magnitude and variable phase response profiles. Magn Reson Med. 1995; 33:648–655. [PubMed: 7596268]
23. Pickup S, Popescu M. Efficient design of pulses with trapezoidal magnitude and linear phase response profiles. Magn Reson Med. 1997; 38:137–145. [PubMed: 9211389]
24. Setsompop K, Wald L, Alagappan V, Gagoski B, Adalsteinsson E. Magnitude least squares optimization for parallel radio frequency excitation design demonstrated at 7 Tesla with eight channels. Magn Reson Med. 2008; 59:908–915. [PubMed: 18383281]
25. Harkins KD, Does MD, Grissom WA. Iterative method for predistortion of MRI gradient waveforms. IEEE Trans Med Imag. 2014; 33:1641–1647.
26. Pauly JM, Le Roux P, Nishimura D, Macovski A. Parameter relations for the Shinnar-Le Roux selective excitation pulse design algorithm. IEEE Trans Med Imag. 1991; 10:53–65.
27. Sharma A, Lustig M, Grissom WA. Root-flipped multiband refocusing pulses. Magn Reson Med. 2016; 75:227–237. [PubMed: 25704154]
28. Sacolick LI, Wiesinger F, Hancu I, Vogel MW. B_1 mapping by Bloch-Siegert shift. Magn Reson Med. 2010; 63:1315–1322. [PubMed: 20432302]
29. Jankiewicz M, Gore JC, Grissom WA. Improved encoding pulses for Bloch-Siegert B1+ mapping. J Magn Reson. 2013; 226:79–87. [PubMed: 23220183]
30. Yip CY, Fessler JA, Noll DC. Iterative RF pulse design for multidimensional, small-tip-angle selective excitation. Magn Reson Med. 2005; 54:908–917. [PubMed: 16155881]
31. Grissom WA, Yip CY, Zhang Z, Stenger VA, Fessler JA, Noll DC. Spatial domain method for the design of RF pulses in multicoil parallel excitation. Magn Reson Med. 2006; 56:620–9. [PubMed: 16894579]
32. Fielden SW, Meyer CH. A simple acquisition strategy to avoid off-resonance blurring in spiral imaging with redundant spiral-in/out k-space trajectories. Magn Reson Med. 2015; 73:704–710. [PubMed: 24604539]

33. Gurney, P., Pauly, JM., Nishimura, DG. A simple method for measuring B0 eddy currents. Proceedings 13th Scientific Meeting, International Society for Magnetic Resonance in Medicine; Miami Beach. 2005. p. 866
34. Pijnappel WWF, van den Boogaart A, de Beer R, van Ormondt D. SVD-based quantification of magnetic resonance signals. J Magn Reson. 1992; 97:122–134.
35. Wilson JL, Jenkinson M, Jezzard P. Optimization of static field homogeneity in human brain using diamagnetic passive shims. Magn Reson Med. 2002; 48:906–914. [PubMed: 12418007]
36. De Graaf RA, Brown PB, McIntyre S, Rothman DL, Nixon TW. Dynamic shim updating (DSU) for multislice signal acquisition. Magn Reson Med. 2003; 49:409–416. [PubMed: 12594742]
37. Juchem C, Nixon TW, McIntyre S, Boer VO, Rothman DL, de Graaf RA. Dynamic multi-coil shimming of the human brain at 7T. J Magn Reson. 2011; 212:280–288. [PubMed: 21824794]
38. Stockmann JP, Witzel T, Keil B, Polimeni JR, Mareyam A, LaPierre C, Setsompop K, Wald LL. A 32-channel combined RF and B_0 shim array for 3T brain imaging. Magn Reson Med. 2016; 75:441–451. [PubMed: 25689977]
39. Yip CY, Fessler JA, Noll DC. Advanced three-dimensional tailored RF pulse for signal recovery in T2∗-weighted functional magnetic resonance imaging. Magn Reson Med. 2006; 56:1050–1059. [PubMed: 17041911]
40. Yang C, Deng W, Alagappan V, Wald LL, Stenger VA. Four-dimensional spectral-spatial RF pulses for simultaneous correction of B1+ inhomogeneity and susceptibility artifacts in T2∗-weighted MRI. Magn Reson Med. 2010; 64:1–8. [PubMed: 20577982]
41. Malik SJ, Larkman DJ, O'Regan DP, Hajnal JV. Subject-specific water-selective imaging using parallel transmission. Magn Reson Med. 2010; 63:988–997. [PubMed: 20146394]
42. Katscher U, Börnert P, Leussler C, van den Brink JS. Transmit SENSE. Magn Reson Med. 2003; 49:144–150. [PubMed: 12509830]
43. Zhu Y. Parallel excitation with an array of transmit coils. Magn Reson Med. 2004; 51:775–784. [PubMed: 15065251]
44. Conolly S, Pauly J, Nishimura D, Macovski A. Two-dimensional selective adiabatic pulses. Magn Reson Med. 1992; 24:302–313. [PubMed: 1569869]
45. Star-Lack J, Nelson S, Kurhanewicz J, Huang L, Vigneron D. Improved water and lipid suppression for 3D PRESS CSI using RF band selective inversion with gradient dephasing (BASING). Magn Reson Med. 1997; 38:311–321. [PubMed: 9256113]
46. Schricker AA, Pauly JM, Kurhanewicz J, Swanson MG, Vigneron DB. Dualband spectral-spatial RF pulses for prostate MR spectroscopic imaging. Magn Reson Med. 2001; 46:1079–1087. [PubMed: 11746572]
47. Cunningham C, Vigneron D, Chen A, Xu D, Hurd R, Sailasuta N, Pauly J. Design of symmetric-sweep spectral-spatial RF pulses for spectral editing. Magn Reson Med. 2004; 52:147–153. [PubMed: 15236378]
48. Cunningham CH, Vigneron DB, Marjanska M, Chen AP, Xu D, Hurd RE, Kurhanewicz J, Garwood M, Pauly JM. Sequence design for magnetic resonance spectroscopic imaging of prostate cancer at 3 T. Magn Reson Med. 2005; 53:1033–1039. [PubMed: 15844147]
49. Xu D, Cunningham CH, Chen AP, Li Y, Kelley DA, Mukherjee P, Pauly JM, Nelson SJ, Vigneron DB. Phased array 3D MR spectroscopic imaging of the brain at 7 T. Magn Reson Imaging. 2008; 26:1201–1206. [PubMed: 18486386]
50. Balchandani P, Pauly J, Spielman D. Interleaved narrow-band PRESS sequence with adiabatic spatial-spectral refocusing pulses for 1H MRSI at 7T. Magn Reson Med. 2008; 59:973–979. [PubMed: 18429014]
51. Feldman RE, Balchandani P. A semiadiabatic spectral-spatial spectroscopic imaging (SASSI) sequence for improved high-field MR spectroscopic imaging. Magn Reson Med. 2016; 76:1071–1082. [PubMed: 26519948]

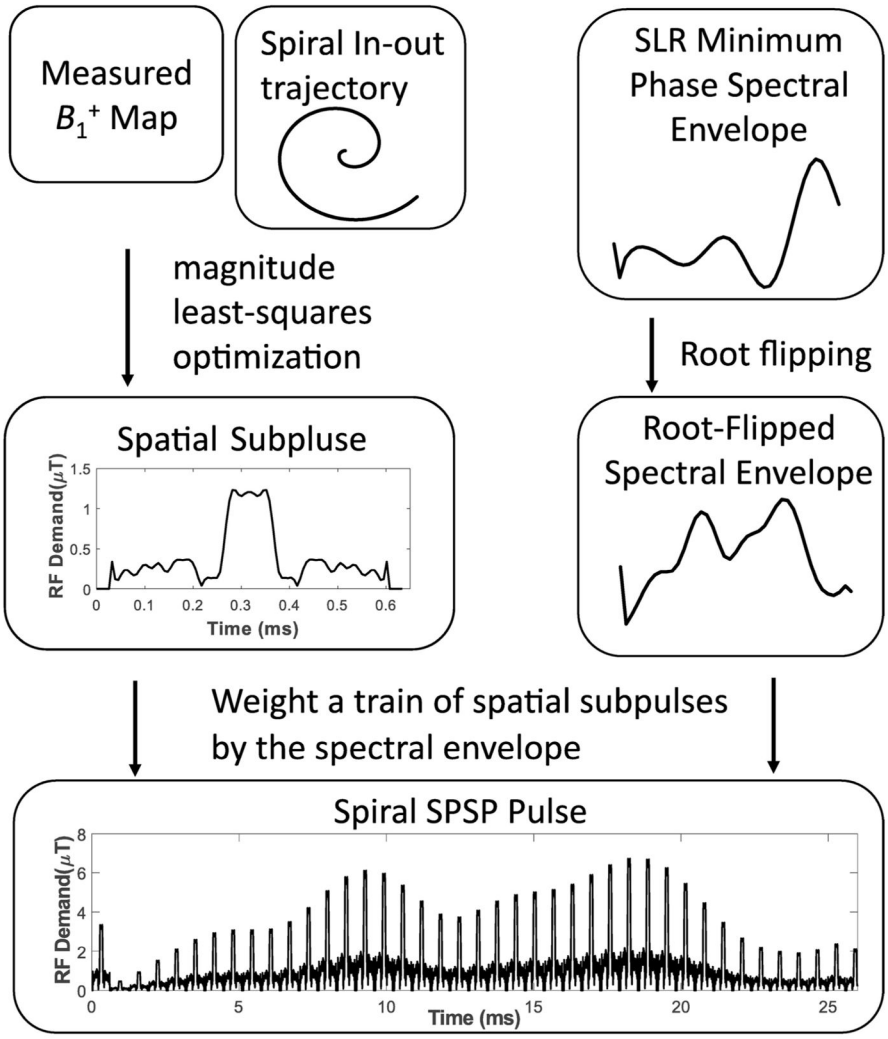

Figure 1.
Overview of tailored spiral in-out SPSP pulse design.

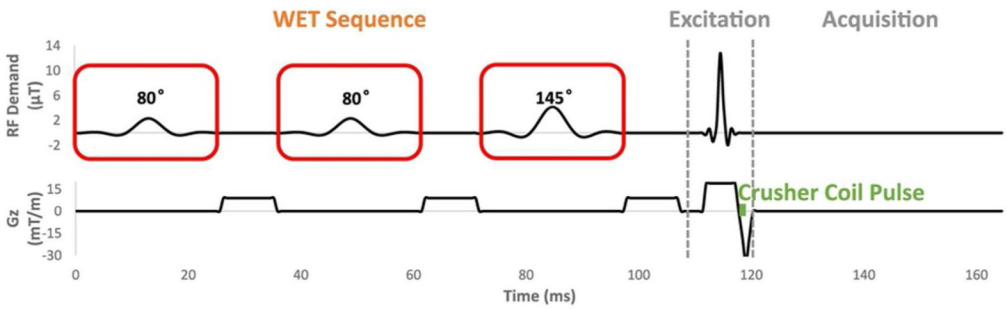

Figure 2.

The WET water suppression sequence, followed by excitation and acquisition for MRSI measurement. Each spectrally-selective excitation pulse is followed by a crusher gradient. The excitation pulses have 80-80-145 degree flip angles, to mitigate the effects of B_1^+ inhomogeneity and T_1 relaxation. In this work, the conventional excitation pulses are replaced with tailored SPSP spiral in-out RF and gradient waveforms, to reduce water suppression errors due to B_1^+ inhomogeneity. The timing of the 1.2 ms crusher coil pulse for skull lipid suppression is indicated.

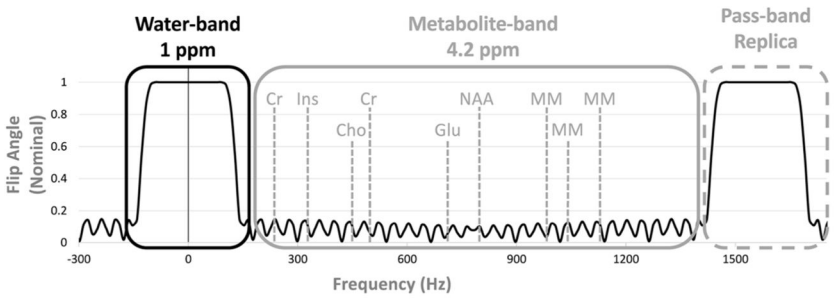

Figure 3.

Frequency profile of the spectral envelope. The spectral FOV is 5.2 ppm, with 1 ppm pass-band and transient-band, and 4.2 ppm stop-band. The pass-band replica does not overlap with the metabolites of interest.

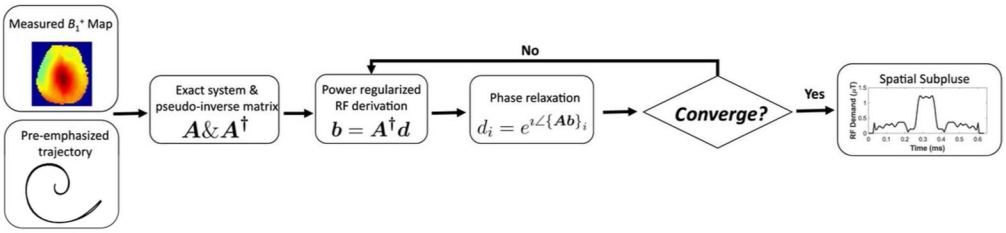

Figure 4.

Patient-tailored spatial subpulse design flowchart. With a patient-dependent B_1^+ map and a pre-emphasized spiral in-out trajectory, the system matrix $\boldsymbol{A}$ is constructed and its RF power-regularized pseudo-inverse $\boldsymbol{A}^\dagger$ is calculated. An iterative magnitude-least-squares optimization is then performed, which interleaves RF pulse calculation with phase relaxation.

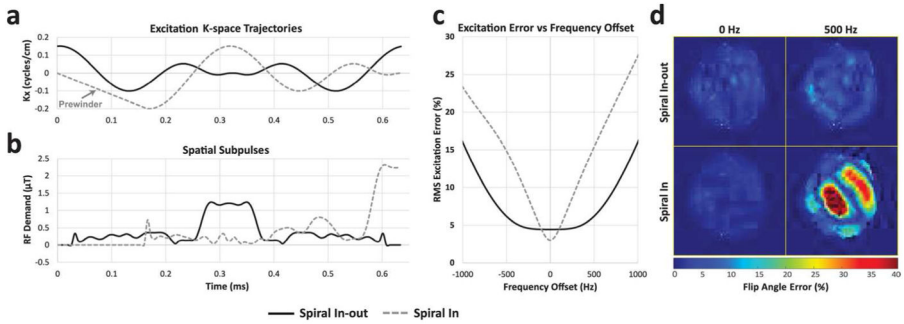

Figure 5.

Spiral in versus spiral in-out subpulse simulations. (a) 0.645 ms spiral-in and spiral in-out k_x trajectories. The initial linear ramp prewinder of the spiral-in trajectory is labeled. (b) Amplitude waveforms of spiral-in and spiral in-out RF subpulses for a human subject. The spiral-in waveform is zero during its prewinder, and the spiral in-out waveform is zero during the up and down ramps at either end of the pulse. (c) RMS excitation error as a function of offset frequency for spiral in and spiral in-out pulses. (d) Percent flip angle error maps at 0 Hz and 500 Hz frequency offset.

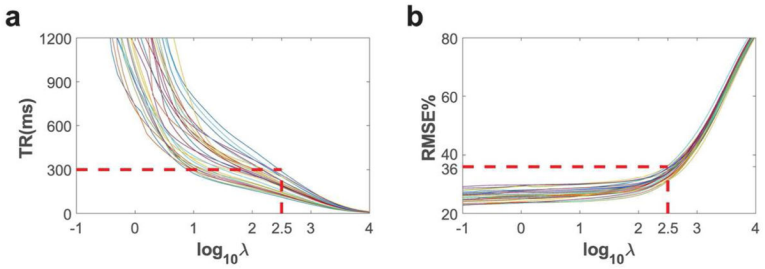

Figure 6.

TR (a) and Root-mean-square excitation error (b) simulated against pulses designed with different RF power regularization parameter λ. Each line represents pulses designed for one of the 28 subjects using B_1^+ maps of slice of interest. When λ equals $10^{2.5}$, designs for all subjects have TR within 300 ms and RMSE within 36%.

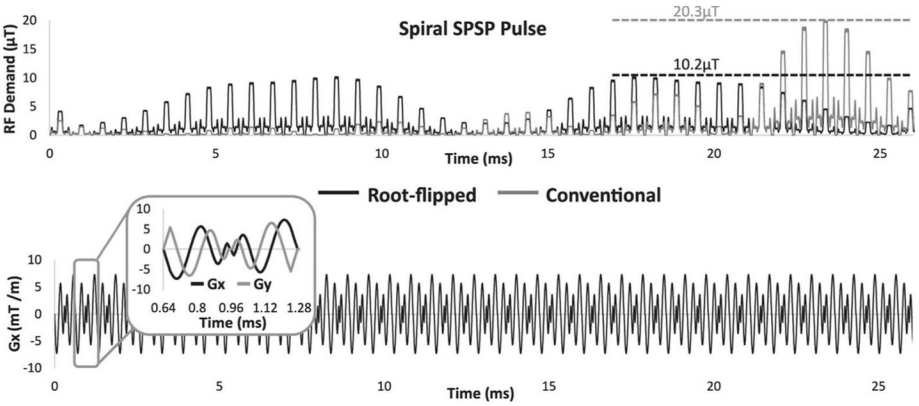

Figure 7.

145 degree RF and x-gradient waveforms designed for a human subject. Root-flipping the spectral envelope reduced peak amplitude by 50% compared to the initial SLR envelope.

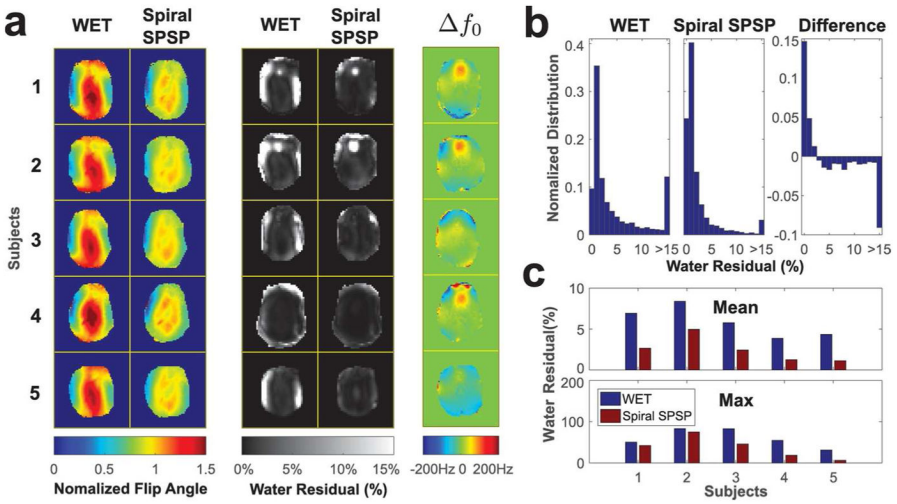

Figure 8.

Comparison of water residuals after conventional and spiral SPSP WET water suppression, in five healthy subjects. (a) Simulated spatial subpulse flip angle maps, water residual maps, and off resonance maps. (b)Water residual histograms across all subjects. (c) Mean and maximum water residuals in each subject.

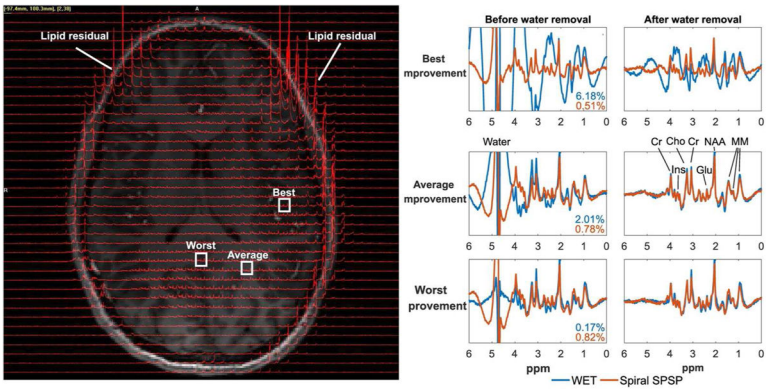

Figure 9.

Subject 3 spectra, acquired with conventional WET and the proposed spiral in-out SPSP water suppression. (Left) Subject 3 spectra acquired with the spiral SPSP water suppression, overlaid on a gradient echo image. Representative voxels are labeled where the spiral SPSP suppression achieved its best, average, and worst improvement compared to conventional WET, in terms of water residual ratios. (Right) The spectra in the three boxed voxels are shown before and after water removal, with percentage water residuals resulting from both methods indicated. All y-axes are unit-less signal intensity and scaled the same.